Available online at www.sciencedirect.com

ScienceDirect

Procedia Computer Science 96 (2016) 1011 – 1021

Procedia Computer Science

20th International Conference on Knowledge Based and Intelligent Information and Engineering Systems

Automatic Detection and Quantification of Abdominal Aortic Calcification in Dual Energy X-Ray Absorptiometry

Karima Elmasri[a*], Yulia Hicks[a], Xin Yang[a], Xianfang Sun[b], Rebecca Pettit[c]

William Evans[c]

[a]*School of Engineering, Cardiff University, Queen's Buildings, Cardiff CF24 3AA ,UK*
[b]*School of Computer Science and Informatics, Cardiff University, Queen's Buildings, Cardiff CF24 3AA, UK*
[c]*Medical Physics and Clinical Engineering, Cardiff and Vale University Health Board, University Hospital of Wales, Cardiff CF14 4XW, UK*

Abstract

Cardiovascular disease (CVD) is a major cause of mortality and the main cause of morbidity worldwide. CVD may lead to heart attacks and strokes and most of these are caused by atherosclerosis; this is a medical condition in which the arteries become narrowed and hardened due to an excessive build-up of plaque on the inner artery wall. Arterial calcification and, in particular, abdominal aortic calcification (AAC) is a manifestation of atherosclerosis and a prognostic indicator of CVD. In this paper, a two-stage automatic method to detect and quantify the severity of AAC is described; it is based on the analysis of lateral vertebral fracture assessment (VFA) images. These images were obtained on a dual energy x-ray absorptiometry (DXA) scanner used in single energy mode. First, an active appearance model was used to segment the lumbar vertebrae L1-L4 and the aorta on VFA images; the segmentation of the aorta was based on its position with respect to the vertebrae. In the second stage, feature vectors representing calcified regions in the aorta were extracted to quantify the severity of AAC. The presence and severity of AAC was also determined using an established visual scoring system (AC24). The abdominal aorta was divided into four parts immediately anterior to each vertebra, and the severity of calcification in the anterior and posterior walls was graded separately for each part on a 0-3 scale. The results were summed to give a composite severity score ranging from 0 to 24. This severity score was classified as follows: mild AAC (score 0-4), moderate AAC (score 5-12) and severe AAC (score 12-24). Two classification algorithms (k-nearest neighbour and support vector machine) were trained and tested to assign the automatically extracted feature vectors into the three classes. There was good agreement between the automatic and visual AC24 methods and the accuracy of the automated technique relative to visual classification indicated that it is capable of identifying and quantifying AAC over a range of severity.

Peer-review under responsibility of KES International

Keywords: Abdominal aortic calcification (AAC); segmentation; active appearance model (AAM), dual energy x-ray absortiometry (DXA).

Peer-review under responsibility of KES International
doi:10.1016/j.procs.2016.08.116

* Corresponding author. Tel.: *E-mail address:* elmasrikm@cardiff.ac.uk

1. Introduction

Cardiovascular disease (CVD) may lead to heart attacks and strokes and it is a major cause of mortality and the main cause of morbidity worldwide. The most prevalent form of CVD is a condition called atherosclerosis, in which the arteries become narrowed and hardened due to an excessive build-up of plaque on the inner artery wall. More than 50% of patients with atherosclerosis die without prior clinical symptoms[1]. Arterial calcification and, in particular, abdominal aortic calcification (AAC) is a manifestation of atherosclerosis and a predictor of CVD[2]. The presence of AAC means that is it very likely that there is some atherosclerosis in the largest artery and elsewhere in the arterial system.

Different imaging modalities have been used to detect and quantify arterial calcification; these include ordinary projection radiography and x-ray computed tomography (CT)[3]. Dual energy x-ray absorptiometry (DXA) is a standard diagnostic technique that is widely used to diagnose and monitor osteoporosis through the measurement of bone mineral density (BMD). Modern DXA scanners are capable of vertebral fracture assessment (VFA) imaging in the lateral projection to detect vertebral fractures, which are a strong indicator of established osteoporosis. However, VFA images can also reveal AAC and it has been suggested that this technique may have a dual role in assessing CVD as well as osteoporosis[4]. It has been shown that VFA can identify AAC with good sensitivity and specificity compared with standard lateral spine radiographs[5,11]. However, studies relating to the risk of cardiovascular events are relatively scant and few have focused directly on AAC.

Several manual quantification methods of the severity of AAC as seen on standard lateral radiographs have been described. An established and validated visual approach is that of Kauppila et al.[6], in which calcification in the walls of the abdominal aorta is scored on a scale ranging from 0 to 24. This method is known as AC24 and it was applied by the Framingham study group[7-9] to estimate CVD risk from lumbar aortic radiographs. The same scoring system was utilised by Mohammad et al.[10] who used the scores to classify AAC as mild, moderate or severe.

Work has also been done on automatic methods of image analysis for the diagnosis of CVD so that a large number of cases may be handled with the same accuracy and high efficiency. A robust algorithm for the delineation of anatomical structures and other regions of interest is crucial for successful automation. Standard image segmentation methods include thresholding, region growing, clustering, classifiers, Markov random field (MRF) models, artificial neural networks, deformable models and atlas-guided approaches. As regards detecting and quantifying ACC on ordinary radiographs, de Bruijne[13] combined pixel classification based on local image structure with a spatially varying prior derived from a statistical model of the combined shape variation in the aorta and the spine. However, the method used one threshold for the entire dataset, which is not applicable in many cases (including the work described in this paper). In another study[20], the severity of atherosclerotic plaque in standard radiographic images was assessed by applying an in-painting technique to remove the plaque followed by an estimation of image background for uncalcified aorta. The main disadvantage of this approach was the fact that manual segmentation influenced the in-painting process.

This paper describes a method for automatic quantification of AAC on VFA images produced by a Discovery A DXA scanner (Hologic, Bedford MA, USA) used in single energy mode, although the DXA manufacturer uses the term instant vertebral assessment (IVA) instead of VFA. An automated method for AAC detection and quantification is likely to be more precise than manual methods. A statistical shape and appearance model of the lumbar spine and the abdominal aorta was built using 20 clinical VFA images from a hospital osteoporosis service. A searching active appearance model (AAM) algorithm[12] was used to fit the built model to the two objects (spine and aorta) in another 53 unseen VFA images. Extracted information was used for automated quantification of AAC in the entire data set of 73 images. To evaluate the accuracy of the automatic method, the classification of features extracted from the segmented aortas was compared with a classification based on the visual AC24 scoring method. All image processing was done in Matlab (MathWorks, Natick MA, USA).

The remainder of the paper is organised as follows. Section 2 describes automatic segmentation using AAM. In the same section, a method for extracting and quantifying AAC is given. In Section 3, AAC classification using the manual AC24 system is described while automatic classification with two classifier algorithms is discussed in

Section 4. A comparison of the results of manual and automatic classification is presented in Section 5 while discussion and a conclusion are given in Section 6.

Approval for the study was obtained from the Cardiff University School of Engineering Ethics Committee.

2. Modelling and Feature Extraction

2.1. Data set

A set of 73 anonymised VFA images of the lateral spine of patients referred for the investigation of osteoporosis at the University Hospital of Wales, Cardiff were obtained. The selected images had different degrees of aortic calcification ranging from mild to severe.

2.2. Building the shape and appearance models

An appearance model (AAM) was implemented, by creating the shape, appearance and combined shape and appearance model using 20 VFA images with clear evidence of aortic calcification selected as a training set. For each image in the training set, landmarks were positioned manually at the corners and at the centre of the end-plates of each of the first four lumbar vertebrae (L1-L4). A further 32 landmarks were placed along the anterior and posterior walls of the calcified aorta adjacent to L1-L4, making 56 landmarks in total. These were used to build the shape and appearance models and as references for search results. Fig. 1 shows an example of an original VFA image (a) and a cropped image with landmarks (b). The shapes were then aligned using a Procrustes algorithm to minimise the sum of the distance of each shape from the mean.

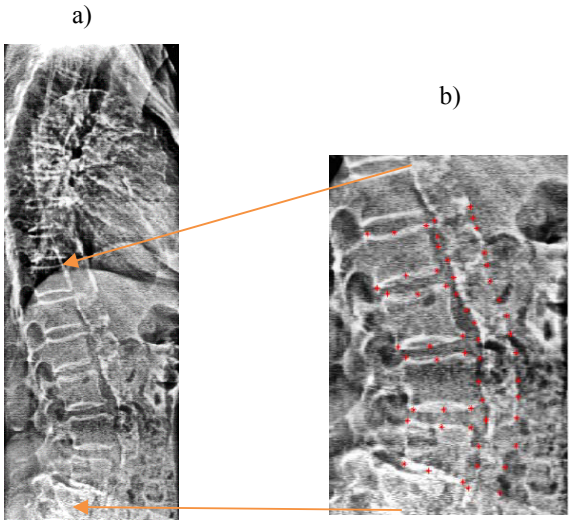

Fig. 1. Example of an annotated VFA image with 56 landmarks (shown as red dots): (a) original image; (b) cropped image with landmarks.

Following this, the mean shape $\bar{x}$ was computed by averaging the position vectors of all landmarks. Principal component analysis (PCA)[14] was performed to calculate the principal modes of variation p_s and their variance λ_s. After PCA, a new approximated vector was produced using:

$$x = \bar{x} + p_s b_s \quad (1)$$

where p_s represents the matrix of ordered eigenvectors and b_s is a set of shape parameters. In the implementation, 10 principal components described 98% of the shape variation.

The statistical appearance model was formed in three steps: obtaining the pixel information, normalising the data to minimise the effect of global brightness variation and modelling the normalised texture variation. The pixel information was captured using a piecewise affine warp based on the Delaunay triangulation[19]. By applying PCA, the texture variation was extracted. Any texture example can be created by deforming the mean pixel value $\bar{g}$ by a linear combination of eigenvectors:

$$g = \bar{g} + p_g b_g \tag{2}$$

where g is the pixel value, b_g is a set of texture parameters and p_g represents the matrix of ordered eigenvectors[15]. Thus, the shape and appearance of any training example of the modelled object can be identified by the two vectors b_s and b_g. Therefore, for every training vector a new concatenated vector was generated:

$$b = \begin{pmatrix} W_s b_s \\ b_g \end{pmatrix} = \begin{pmatrix} W_s p_s^T (x - \bar{x}) \\ p_g^T (g - \bar{g}) \end{pmatrix} \tag{3}$$

where W_s is the diagonal matrix of weights for each shape parameter, to give appropriate balance between the shape and the texture models. Applying PCA on this vector yielded a new further model:

$$b = p_c c \tag{4}$$

where p_c are the eigenvectors and c is a vector of appearance parameters controlling both the shape and grey-levels of the model.

2.3. Active appearance model (AAM) searching algorithm

To find the two objects (lumbar spine and aorta), the searching AAM developed by Cootes et al.[12] was used to fit the produced statistical shape and appearance model to new set of 53 unseen VFA images. The mean shape produced was placed in an approximate correct position on a VFA image. The algorithm was then used to fit spine and aorta edges. To see how the AAM can fit the data, leave-one-out tests were carried out on all images in the dataset. Fig. 2 shows the searching process using the AAM.

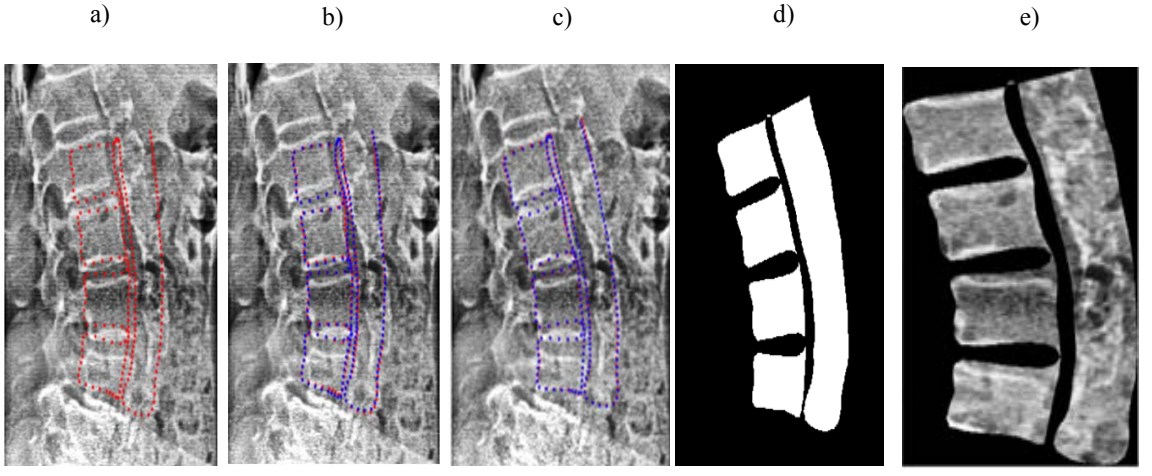

Fig. 2. Application of the searching active appearance model: (a) initial position; (b) and (c) finding the best fit; (d) segmented spine and aorta in binary scale; (e) segmented spine and aorta at the end of the searching process.

2.4. Extracting the aorta from the segmented image

In order to extract the aorta from the segmented image produced by the AAM, a connected component labelling algorithm based on pixel connectivity was implemented. The algorithm works by scanning an image pixel-by-pixel (from top to bottom and left to right) in order to identify connected pixel regions. Thus, equivalent label pairs were sorted into equivalence classes and a unique label was assigned to each class. This was done for all of the 73 VFA images in the data set. The aorta was extracted as the labelled object that had the greatest area in the entire image; all other objects related to the background and the spine were removed.

Fig. 3 shows the extracted aorta for the example shown in Fig. 2. Further examples of calcified aortas extracted from various segmented images produced from the AAM are presented in Fig. 4.

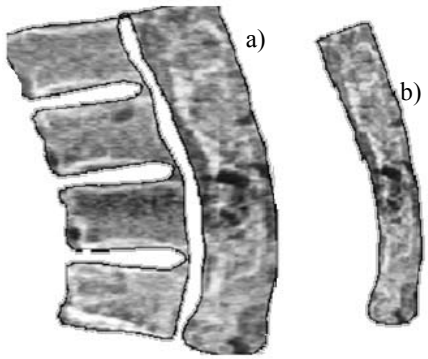

Fig. 3. Extracting the aorta: (a) segmented spine and calcified aorta produced by the AAM; (b) object with the greatest area (aorta).

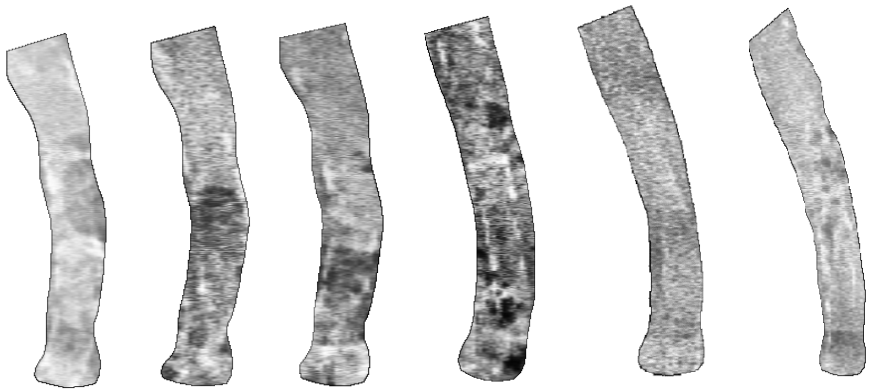

Fig. 4. Examples of segmented calcified aortas.

2.5. Image Quantisation

Although the segmented aorta obtained from the AAM clearly masked out all the calcified pixels, sometimes it also detected parts of the aorta that had high brightness due to changes in soft tissue composition. This variation in brightness and the influence of obesity made the use of a single threshold not applicable in the next stage. Multilevel thresholding is a technique that segments a grey level image into several distinct regions[17]. The technique defines more than one threshold for the specified image and it segments the image into regions of certain brightness that identify the background and several objects. In the application of multilevel thresholding, every segmented aorta was processed using specified quantisation levels and output values.

The number of optimal thresholds was assigned by calculating the peak signal-to-noise ratio (PSNR) for each segmented aorta[17]. Fig. 5 shows that for three different examples of aorta with low, moderate and high calcification, the PSNR reached saturation after seven threshold levels. As the number of thresholds increased, the thresholded image tended towards the original image and this was evaluated visually. An example of a quantised image with different threshold levels is presented in Fig. 6. It is clear that after 14 levels of thresholding, the image (f) tended towards the original (a).

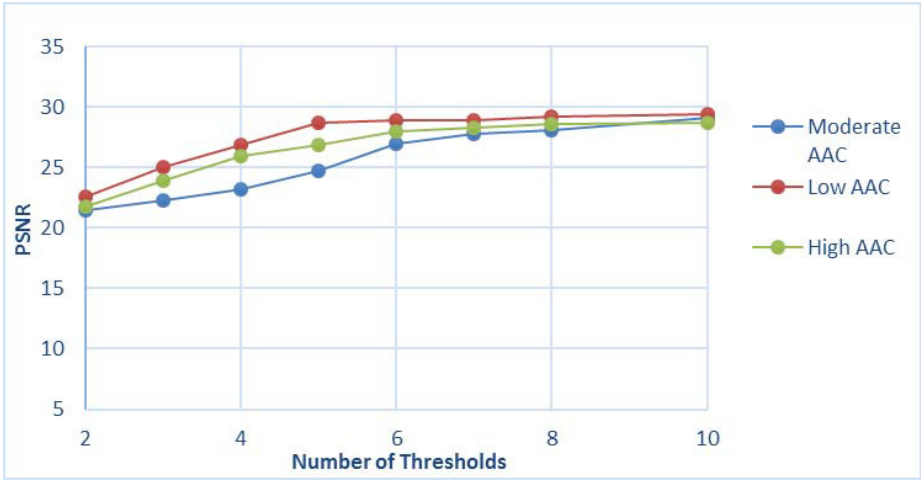

Fig. 5. Plots of PSNR vs. number of thresholds for three different calcified aortas: moderate AAC; low AAC; high AAC.

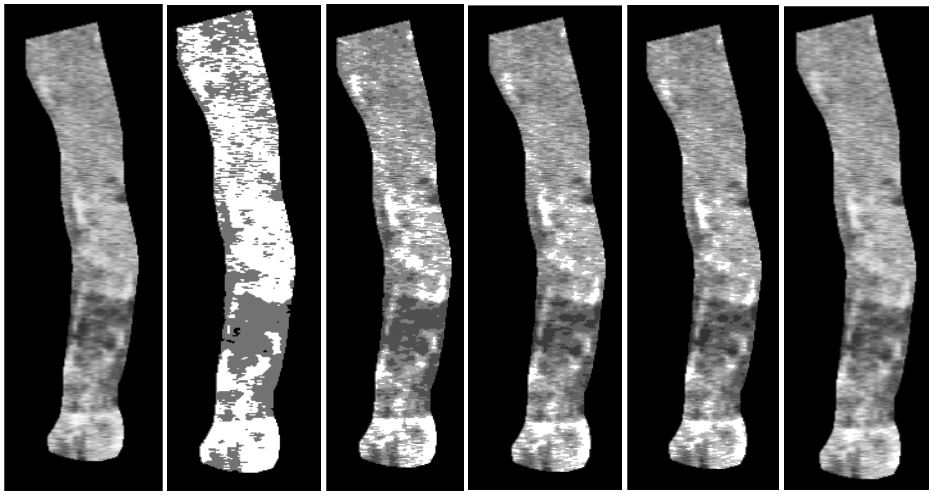

a) b) c) d) e) f)

Fig. 6. Image quantisation: (a) original aorta image; (b) 2-level thresholding; (c) 4-level; (d) 6-level; (e) 7-level; (f) 14-level.

2.6. Feature Extraction

First-order texture analysis was implemented to extract the features of every segmented aorta. The main advantage of this approach is the simplicity of using standard descriptors (e.g. mean and variance). Regions that did not represent calcification in the aorta were removed empirically. Over the entire set of quantised images of the segmented aorta, the area of these regions varied from 10 to 80 pixels. For automatic removal of these regions, an average area of 50 pixels was used. The ratio of the number of calcified pixels to the total number of pixels in each aorta was the first feature extracted. In order to capture the spatial dependence of grey-level values, which contribute to the perception of texture, a grey-level co-occurrence matrix (GLCM) was computed for every quantised aorta image. Seven features commonly used to describe the properties of the image histogram were extracted: mean, variance, energy, entropy, homogeneity, contrast and correlation.

Thus a total of 8 features were extracted for each of the 73 aorta images. Fig. 7 shows an example of a calcified aorta after quantisation and thresholding to reveal pixels containing calcification. In this case, the binary image shown in Fig. 7(c) was used to calculate the ratio feature.

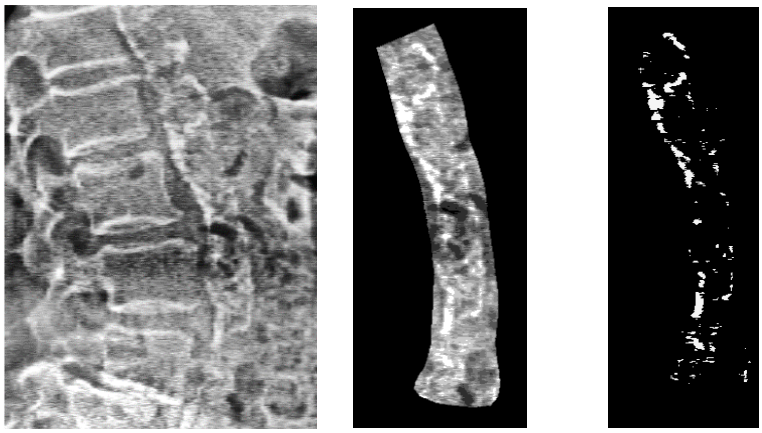

Fig. 7. Feature extraction: (a) original image; (b) segmented aorta quantised using 7 levels; (c) binary image after thresholding.

3. Manual Calcification Scoring and Classification

To validate the accuracy of the automatic technique, aortic calcification on the VFA images was scored visually using the AC24 method[6,8] by one observer as shown in Fig. 8. For each image, the abdominal aorta was divided into four parts immediately anterior to each of the lumbar vertebrae L1-L4. For each part, aortic calcification severity in the anterior and posterior longitudinal walls was graded separately on a 0-3 scale: 0 for no AAC; 1 for small, scattered calcified deposits occupying less than ⅓ of the wall length; 2 for deposits occupying more than ⅓ but less than ⅔ of the wall length and 3 if ⅔ or more of the wall length was calcified. The results were summed to give a composite severity score ranging from 0 to 24. Subsequently, the approach of Mohammad et al.[10] was used to

classify AAC as follows: mild AAC (score 0-4), moderate AAC (score 5-12) and severe AAC (score >12). Table1 shows the AC24 scoring for the example shown in Fig. 8.

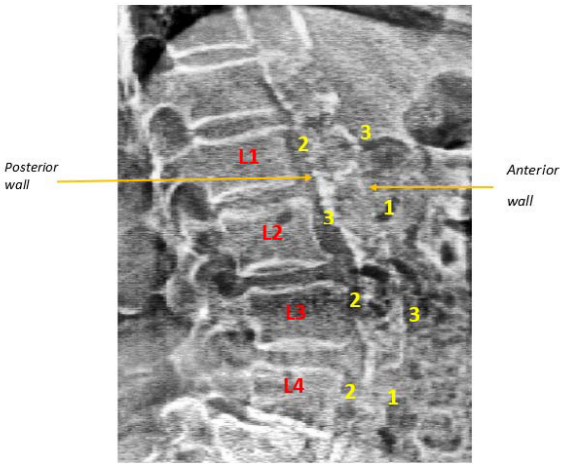

Fig. 8. Labelled image with AC24 score points.

Table 1. An example of AC24 scoring for one VFA image of the aorta.

Vertebral Level	AC24 scores Anterior wall (0-3)	Posterior wall (0-3)	Anterior + Posterior (0-6)
L1	2	3	5
L2	3	1	4
L3	2	3	5
L4	2	1	3
Sum	9	8	17
Maximum	12	12	24

4. Automatic Calcification Classification

Two classifiers were tested to evaluate the automatic method for AAC quantification against visual scoring. The first was k-nearest neighbour (k-NN) as used by de Bruijne[13]. The second was a support vector machine (SVM) using a linear kernel function from LIBSVM (a Library for Support Vector Machines). A K-folds cross validation method was implemented with 5 folds to partition the data set into two parts: a set to train the classification model and a set to validate the model. The output of this implementation was the assignment of each aorta image into one of three classes based on the values of the extracted features. Again, the three classes used were as follows: class 1 for mild AAC, class 2 for moderate AAC and class 3 for severe AAC.

4.1 Feature selection

In general, the performance of any automatic classifier is not optimised when all features are used. In order to assess the relative importance of the 8 extracted features, s-fold cross-validation[18] was utilised as a feature selection algorithm to obtain correct classification rates (CCR). Fig. 9 shows the CCR for the individual features: 1 ratio of calcified area/total area, 2 entropy, 3 variance, 4 energy, 5 correlation, 6 mean, 7 contrast and 8 homogeneity.

The three optimum features were the area ratio, entropy and variance; these had CCR values of 0.977, 0.963 and 0.923 respectively. CCR deteriorated for the other features; contrast and homogeneity had the worst CCR values of 0.746 and 0.694 respectively. In practice, the k-NN and SVM classifiers used an appropriate combination of features for image classification.

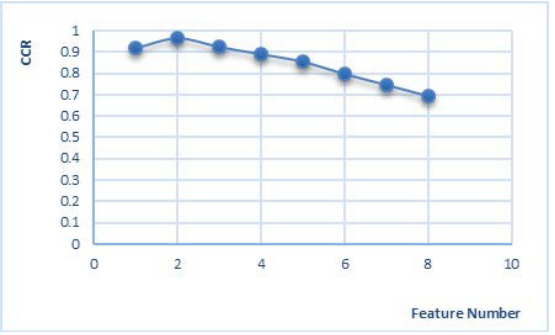

Fig. 8. Variation of CCR with feature number.

5. Comparison of Automatic and Visual Classification

The results of automatic AAC classification compared with visual classification are shown in Fig. 10. The accuracy of k-NN (93.1%, 90.4% and 95.2% for classes 1, 2 and 3 respectively) was better than that of SVM (87.7%, 83.3% and 94.5%) as shown in Fig. 10(a). The performance of the two automatic classifiers was also assessed by receiver operating characteristic (ROC) analysis. Fig 10(b) shows the area under the curve (AUC) of sensitivity vs. (1 – specificity) for each classifier. Similar performance was found for all classes.

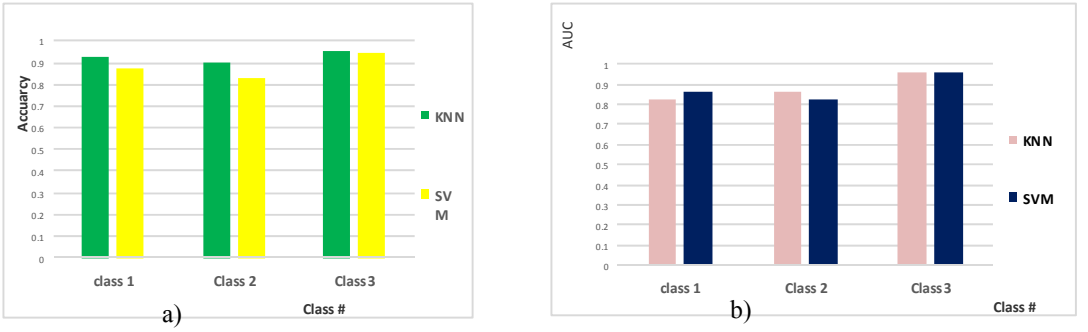

Fig. 10. Comparison of automatic and visual classification: (a) accuracy of k-NN and SVM classifiers for AAC classes 1, 2 and 3; (b) AUC for each classifier and AAC class.

6. Discussion and Conclusion

In this work, the severity of abdominal aortic calcification was measured automatically on single energy vertebral fracture assessment images acquired on a dual energy x-ray absorptiometry scanner. This confirms that VFA imaging with a bone densitometer can simultaneously detect prevalent vertebral fracture, a strong indicator of prevalent osteoporosis, and abdominal AAC, which is an important risk factor for cardiovascular disease.

The automatic method comprised two stages. In the first stage an active appearance model was employed for automatic segmentation. The novelty and advantage of the current study is that the active appearance model used here was based on training images originating from patients undergoing DXA for the diagnosis and monitoring of osteoporosis. The model was trained on 20 VFA images and tested on another 53 unseen VFA images. AAM was able to extract two relevant objects (the aorta and the spine) with high accuracy; the method was robust and it took only few seconds to complete the searching process.

To quantify AAC automatically, a new method based on feature extraction was developed. This was validated against an established manual technique (AC24) using k-NN and SVM as classifiers. For the selected data set of 73 images, the automatic method achieved high accuracy for all classes of AAC severity. This suggests that this approach may assist in the identification of patients with atherosclerosis before symptoms of cardiovascular disease develop.

In the future, the work will be extended to include VFA images from patients who have little or no aortic calcification.

7. Acknowledgements

We thank Ali Khayeat and Mahmud Abdulla, postgraduate students at Cardiff University, for their technical assistance.

References

1. Barascuk N, Ganz M, Nielsen M, Register TC, Rasmussen LM, Karsdal MA, Christiansen C. Abdominal aortic calcification quantified by the Morphological Atherosclerotic Calcification Distribution (MACD) index is associated with features of the metabolic syndrome. *BMC Cardiovascular Disorders* 2011; **11**: 75-83.
2. Cecelja M, Frost ML, Spector TD, Chowienczyk P. Abdominal aortic calcification detection using dual-energy x-ray absorptiometry: validation study in healthy women compared to computed tomography. *Calcified Tissue International* 2013; **92**: 495-500.
3. Jayalath RW, Mangan SH, Golledge J. Aortic calcification. *European Journal of Vascular and Endovascular Surgery* 2008; **30**: 476-488.
4. Wilson KE. Detection of abdominal aortic calcification with IVA. Bedford MA, USA: Hologic Inc.; 2006.
5. Golestani R, Tio RA, Zeebregts TJ, Zeilstra A, Dierckx RA, Boersma HH, Hillege HL, Slart RHJA. Abdominal aortic calcification detected by dual x-ray absorptiometry: a strong predictor for cardiovascular events. *Annals of Medicine* 2010; **42**: 539–545.
6. Kauppila LI, Polak JF, Cupples LA, Hannan MT, Kiel DP, Wilson PWF. New indices to classify location, severity and progression of calcific lesions in the abdominal aorta: a 25-year follow-up study. *Atherosclerosis* 1997; **132**: 45–50.
7. Witteman JCM, Kok FJ, van Saase JLCM, Valkenburg HA. Aortic calcification as a predictor of cardiovascular mortality. *Lancet* 1986; **328**: 1120–1122.
8. O'Donnell CJ, Chazaro I, Wilson PWF, Fox C, Hannan MT, Kiel DP, Cupples LA. Evidence for heritability of abdominal aortic calcific deposits in the Framingham Heart Study. *Circulation* 2002; **106**: 337–341.
9. Ganz M, de Bruijne M, Dam E, Pettersen P, Karsdal MA, Christiansen C, Nielsen M. Distribution, size and shape of abdominal aortic calcified deposits and their relationship to mortality in postmenopausal women. *International Journal of Biomedical Imaging* 2012; **2012**: 1-8.
10. Mohammad A, Lohan D, Bergin D, Mooney S, Newell J, O'Donnell M, Amin S, Coughlan RJ, Carey JJ. Vertebral fracture assessment-detected abdominal aortic calcification and cardiovascular disease in rheumatoid arthritis. *Seminars in Arthritis and Rheumatism* 2014; **43**: 632-637.
11. Higgins CL, Marvel SA, Morrisett JD. Quantification of calcification in atherosclerotic lesions. *Arteriosclerosis, Thrombosis, and Vascular Biology* 2005; **25**: 1567–1576.
12. Cootes TF, Edwards GJ, Taylor CJ. Active appearance models. *IEEE Transactions on Pattern Analysis and Machine Intelligence* 2001; **23**: 681–685.
13. de Bruijne M. A pattern classification approach to aorta calcium scoring in radiographs. In: Liu Y, Jiang T, Zhang C, editors. *Computer vision for biomedical image applications*. Berlin: Springer Verlag; 2005. p.170–177.
14. Jolliffe I. Principal component analysis. In: Everitt BS, Howell D, editors. *Encyclopedia of statistics in behavioral science.* Volume 3. Hoboken NJ, USA: John Wiley; 2005. p. 1580–1584.

15. Vasconcelos MJM, Tavares JMRS. Methodologies to build automatic point distribution models for faces represented in images. In Tavares JM, Natal JRM, editors. *Computational modelling of objects represented in images: fundamentals, methods and applications. Proceedings of the international symposium CompIMAGE*. Bristol PA, USA: Taylor and Francis. 2006. p. 1-6.
16. Burger W, Burge MJ. *Principles of digital image processing - advanced methods*. London: Springer Verlag; 2013.
17. Horng MH, Liou RJ. Multilevel minimum cross entropy threshold selection based on the firefly algorithm. *Expert Systems with Applications* 2011; **38**: 14805–14811.
18. Le D, Provost EM. Emotion recognition from spontaneous speech using hidden Markov models with deep belief networks. In: Hajic J, Hain T, Mercer B, editors. *Proceedings of the IEEE Workshop on Automatic Speech Recognition and Understanding (ASRU) 2013*. Piscataway NJ, USA: IEEE; 2013. p. 216-221.
19. Cootes TF, Taylor, CJ. Statistical models of appearance for medical image analysis and computer vision. In: Sonka M, Hanson KM, editors. *Proceedings of the SPIE Conference on Medical Imaging: Image Processing 2001*. Bellingham WA, USA: SPIE; 2001. p. 1-14.
20. Conrad-Hansen L, de Bruijne M, Lauze F, Tanko LB, Pettersen PC, He Q, Chen J, Christiansen C, Nielsen M. Quantifying calcification in the lumbar aorta on x-ray images. In: Ayache N, Ourselin S, Maeder M, editors. *Medical Image Computing and Computer-Assisted Intervention (MICCAI). Proceedings of the 10th International Conference.* Part 2. Berlin: Springer Verlag; 2007. p. 352-359.